


ORIGINAL PAPER

Morphology of GNAT3-immunoreactive chemosensory cells in the nasal cavity and pharynx of the rat

Yoshio Yamamoto¹  | Takuya Yokoyama² | Nobuaki Nakamuta¹

¹Laboratory of Veterinary Anatomy and Cell Biology, Faculty of Agriculture, Iwate University, Morioka, Japan

²Department of Anatomy (Cell Biology), Iwate Medical University, Yahaba, Japan

Correspondence

Yoshio Yamamoto, Laboratory of Veterinary Anatomy and Cell Biology, Faculty of Agriculture, Iwate University, 18-8 Ueda 3-chome, Morioka, Iwate 020-8550, Japan.
Email: yyoshio@iwate-u.ac.jp

Abstract

Solitary chemosensory cells and chemosensory cell clusters are distributed in the pharynx and larynx. In the present study, the morphology and reflexogenic function of solitary chemosensory cells and chemosensory cell clusters in the nasal cavity and pharynx were examined using immunofluorescence for GNAT3 and electrophysiology. In the nasal cavity, GNAT3-immunoreactive solitary chemosensory cells were widely distributed in the nasal mucosa, particularly in the cranial region near the nostrils. Solitary chemosensory cells were also observed in the nasopharynx. Solitary chemosensory cells in the nasopharyngeal cavity were barrel like or slender in shape with long lateral processes within the epithelial layer to attach surrounding ciliated epithelial cells. Chemosensory cell clusters containing GNAT3-immunoreactive cells were also detected in the pharynx. GNAT3-immunoreactive cells gathered with SNAP25-immunoreactive cells in chemosensory clusters. GNAT3-immunoreactive chemosensory cells were in close contact with a few SP- or CGRP-immunoreactive nerve endings. In the pharynx, GNAT3-immunoreactive chemosensory cells were also attached to P2X3-immunoreactive nerve endings. Physiologically, the perfusion of 10 mM quinine hydrochloride (QHCl) solution induced ventilatory depression. The QHCl-induced reflex was diminished by bilateral section of the glossopharyngeal nerve, suggesting autonomic reflex were evoked by chemosensory cells in pharynx but not in nasal mucosa. The present results indicate that complex shape of nasopharyngeal solitary chemosensory cells may contribute to intercellular communication, and pharyngeal chemosensory cells may play a role in respiratory depression.

KEYWORDS

chemosensory cells, GNAT3, immunohistochemistry, nasal cavity, pharynx, respiratory depression

1 | INTRODUCTION

Solitary chemosensory cells are diffusively distributed in the respiratory epithelium in the nasal cavity, pharynx, larynx, and trachea (for reviews, see Krasteva & Kummer, 2012; Tizzano & Finger, 2013). Previous studies reported that solitary chemosensory cells and chemosensory cells in clusters express Tas1R3, which is one of the taste

receptors related to bitter perception (Tizzano et al., 2011). They also contain taste transduction molecules, such as GNAT3 (α -gustducin), phospholipase C, β 2-subunit (PLC β 2), inositol 1,4,5-trisphosphate receptor type 3 (IP3R3), and TRPM5 (Finger et al., 2003; Merigo et al., 2005; Sbarbati et al., 2004; Tizzano et al., 2011). Functionally, intracellular calcium ion concentrations increased in dissociated chemosensory cells treated with the bitter stimulant, denatonium benzoate

(Gulbransen, Clapp, et al., 2008). Lee et al. (2014) reported that increase in intracellular Ca^{2+} in the sinonasal solitary chemosensory cells activated by bitter stimulant propagate to surrounding respiratory ciliated cells to release anti-bacterial peptide. On the other hand, a stimulation of the nasal mucosa by denatonium benzoate, quinine hydrochloride (QHCl), or cycloheximide induced apnea (Tizzano & Finger, 2013). The perfusion of QHCl into the laryngeal cavity also induced ventilatory depression (Masuda et al., 2019). Thus, the chemosensory cells may participate in local immune system of the upper airway and/or involvement of bitter evoked autonomic reflex.

Morphologically, nasal solitary chemosensory cells are distributed on the nasal mucosa facing nasal airflow and have a slender, elongated, or flask-shaped profile (Finger et al., 2003; Gulbransen, Clapp, et al., 2008; Lin et al., 2008). In the pharynx, solitary chemosensory cells have been found in nasopharyngeal mucosa (Tizzano et al., 2011), and some chemosensory cells cluster and are sometimes referred to as 'taste buds' (Henkin & Christiansen, 1967; Lalonde & Eglitis, 1961; Sekerková et al., 2005; Travers & Nicklas, 1990). According to the innervation, solitary chemosensory cells in the nasal mucosa attached to nerve endings immunoreactive for protein gene product 9.5, substance P (SP), and calcitonin gene-related peptide (CGRP; Finger et al., 2003; Gulbransen, Silver, et al., 2008; Lin et al., 2008; Tizzano et al., 2010, 2011). It has been stated that SP- and/or CGRP-immunoreactive nerve endings may be activated by the activation of the nasal solitary chemosensory cells to induce apnea (Finger et al., 2003; Tizzano et al., 2010). Furthermore, Finger et al (2003) also reported synaptic specialization in the nasal solitary chemosensory cells and synaptic vesicles within the cells. In the larynx, nerve endings immunoreactive for P2X2/P2X3 purinoreceptors were also observed on solitary chemosensory cells (Masuda et al., 2019; Takahashi et al., 2016). Furthermore, numerous chemosensory cell clusters in the larynx were innervated by P2X3-immunoreactive nerve fibers (Masuda et al., 2019). However, the morphology and innervation of chemosensory cells in the nasopharyngeal mucosa have not yet been examined in detail.

In the present study, the morphology and innervation of solitary chemosensory cells and chemosensory cell clusters in the respiratory mucosa of the nasal cavity and pharynx were examined using whole-mount preparations with GNAT3 immunoreactivity. We also investigated cardiorespiratory flexes evoked by the bitter stimulant, QHCl, which was perfused into the nasopharyngeal cavity, in physiological experiments in combination with denervation of the glossopharyngeal nerve (GPN).

2 | MATERIALS AND METHODS

2.1 | Animal procedure

All procedures for animal handling were performed in accordance with the guidelines of the local Animal Ethics Committee of Iwate University (accession number: A201902). Male Wistar rats (8–10 weeks old; $n = 28$) were purchased from Japan SLC, Inc. (Slc: Wistar, Japan SLC).

2.2 | Immunohistochemistry

Details of the antibodies used in the present study and their combinations are shown in Tables 1–3.

Regarding whole-mount preparations, rats ($n = 10$) were anesthetized by an intraperitoneal injection of pentobarbital (150 mg/kg), and transcardially perfused with Ringer's solution (300 ml) followed by 4% paraformaldehyde in 0.1 M phosphate buffer (pH 7.4; 300 ml). The nasal respiratory mucosa was peeled off the nasal septum and concha. To prepare the pharyngeal mucosa, tissues including the pharynx, larynx, and proximal part of the trachea and esophagus were dissected out. The larynx was then removed and peeled off the palate to prepare the oropharynx. The remaining tissues were opened at the dorsal midline and used to prepare the nasopharynx. Methodological difficulties were associated with examining the laryngopharynx in a whole-mount preparation; therefore, cryostat sections were prepared as described below. Whole-mount preparations were incubated with primary antibodies at 4°C for at least 5 days. They were then incubated with secondary antibodies at room temperature for 3 h, followed by an incubation with 4',6-diamidino-2-phenylindole (DAPI) solution (1 µg/ml, Dojindo) at room temperature for 10 min. Preparations were mounted on glass slides and coverslipped with aqueous mounting medium (Fluoromount, Diagnostic Biosystems).

Regarding cryostat sections ($n = 6$), the proximal part of the nasal cavity and tissue blocks from the proximal end of the soft palate to the vocal fold were dissected out and then fixed at 4°C for 12–18 h. Tissues were soaked in phosphate buffered saline (PBS) containing 30% sucrose, frozen at -80°C with compound medium (Tissue-Tek O.C.T. compound, Sakura Finetek), and then sectioned in transverse planes at a thickness of 20 µm. These sections were mounted on glass slides coated with chrome-alum gelatin and dried. After being incubated with normal donkey serum (1:50) at room temperature for 30 min, sections were then incubated with the primary antibody at 4°C for 12 h. Sections were subsequently incubated with secondary antibodies at room temperature for 90 min after rinsing with PBS. Preparations were then incubated with DAPI solution for nuclear staining (1 µg/ml) for 5 min. Sections were coverslipped with aqueous mounting medium.

2.3 | Observations

Preparations were examined under a confocal scanning laser microscope (C2si, Nikon). Images of Alexa488, Cy3, and DAPI were captured and colored using computer software (NIS-Elements, Nikon). Projection images were made from z-stacks of confocal images (10–25 series at 1-µm intervals) using the same software. Other images were reconstructed to a three-dimensional view from binary images converted from the original (Figures 4a-2, 4b-2, 4c-2, 4d-2, 4e-2, 4f-2, and 5d-3) or alpha-blending from intact confocal images of z-stack series (Figures 5e-3, 5e-4, 7a-2, 7b-2, 7c-2, 7d-2, 9a-2, and 9c-3). Digital section views (Figure 5d-2, 5e-2, and 9c-2) were also made.

TABLE 1 Primary antibodies used in the present study

Antibody against	Antigen	Manufacturer; host; catalog number; RRID	Dilution	Function; Immunohistochemical marker for
1 Guanine nucleotide-binding protein G(t) _{subunit} α 3 (GNAT3)	Synthetic peptide (KNQFLDLNLKKEDKE), 304-318 amino acid sequence of human GNAT3	Abcam; goat; ab113664; AB_10866449	1:2,000	Taste signaling protein; Chemosensory cells
2 Synaptosomal-associated protein 25 kD (SNAP25)	Crude human synaptic immunoprecipitate (characterized by Honer et al., 1993)	Bio-Rad; mouse (monoclonal); MCA1308; AB_322417	1:2,000	SNARE protein; Neuroendocrine cells; and certain nerve fibers
3 Phospholipase C, β 2-subunit (PLC β 2)	Synthetic peptide (QDPLIAKADAQ), 1170-1181 amino acid sequence of human PLC β 2	Santa Cruz Biotechnology; rabbit; sc-206; AB_632197	1:500	Taste signaling protein; Chemosensory cells
4 Inositol 1, 4, 5-trisphosphate receptor, type 3 (IP3R3)	Synthetic peptide, 22-230 amino acid sequence of human IP3R3	BD Bioscience; mouse (monoclonal); 610312; AB_397704	1:100	Taste signaling protein; Chemosensory cells
5 Substance P (SP)	Synthetic peptide (RPKPQQFFGLM) entire sequence	EMD-Millipore; rabbit; AB1566; AB_2271494	1:2,000	Neuropeptide C-fiber
6 Calcitonin gene-related peptide	Synthetic peptide corresponding to a portion of rat α -calcitonin gene-related peptide (CGRP)	ENZO Life Sciences; rabbit; BML-CA1134; AB_2068527	1:2,000	Neuropeptide C-fiber
7 Bassoon	Recombinant, rat bassoon fragment (residues 738-1035) expressed as a fusion protein in <i>E. coli</i>	ENZO Life Sciences; mouse; ADI-VAM-PS003; AB_10618753	1:5,000	Scaffold protein Presynaptic active zone
8 P2X3 ATP receptor (P2X3)	Synthetic peptide (VEKQSTDGAYSIGH), 383-397 amino acid sequence of rat P2X3	NeuroMics; rabbit; RA10109; AB_21579930	1:2,000	Ionotropic ATP receptor; Certain sensory nerves

The antibody numbers in this table were also used in Table 3.

TABLE 2 Secondary antibodies used in the present study

	Antibody	Host	Catalog number	RRID	Dilution
a	Alexa Fluor 488-labeled anti-goat IgG	Donkey	705-545-147	AB_2336933	1:200
b	Cy3-labeled anti-rabbit IgG	Donkey	711-165-152	AB_2307443	1:100
c	Cy3-labeled anti-mouse IgG	Donkey	715-165-151	AB_2315777	1:100
d	Alexa Fluor 647-labeled anti-rabbit IgG	Donkey	711-605-152	AB_2492288	1:100
e	Alexa Fluor 647-labeled anti-mouse IgG	Donkey	715-605-150	AB_2340862	1:100

The letters for each antibody in this table were also used in Table 3.

All antibodies were supplied by Jackson ImmunoResearch.

TABLE 3 Combinations of antibodies for immunofluorescence

Combination	Primary antibody 1	Secondary antibody 1	Primary antibody 2	Secondary antibody 2	Primary antibody 3	Secondary antibody 3	
GNAT3	1	a	—	—	—	—	Figures 3, 4, and 5d
GNAT3/SNAP25	1	a	2	c	—	—	Figure 5a–c
GNAT3/SNAP25	1	a	2	e	—	—	Figure 5e
GNAT3/PLC β 2	1	a	3	b	—	—	Figure 6a–c
GNAT3/IP3R3	1	a	4	c	—	—	Figure 6d–f
GNAT3/PLC β 2/IP3R3	1	a	3	d	4	c	Figure 6g–i
GNAT3/SP	1	a	5	b	—	—	Figure 7a,c,f,g
GNAT3/CGRP	1	a	6	b	—	—	Figure 7b,d,e
GNAT3/SP/Bassoon	1	a	5	b	7	e	Figure 8a
GNAT3/CGRP/Bassoon	1	a	6	b	7	e	Figure 8b
GNAT3/P2X3	1	a	7	b	—	—	Figure 9

Numbers and letters are shown in Tables 1 and 2.

2.4 | Physiological experiment

Rats ($n = 12$) were used to record the autonomic reflexes evoked by the application of the bitter stimulant QHCl to the nasopharyngeal cavity (Figure 1). To compare the C-fiber stimulation, capsaicin was used. Rats were anesthetized by an intraperitoneal injection of urethane (1.0 g/kg body weight). The midline of the neck was incised to expose the larynx and trachea, and the esophagus was ligated to prevent swallowing of the test solution. We previously reported that the application of QHCl to the laryngeal mucosa evoked respiratory depression via this nerve (Masuda et al., 2019), thus the superior laryngeal nerve on both sides was then severed near the larynx to prevent such reflex. It has been reported that sensory nerves in the pharyngeal mucosa were innervated by glossopharyngeal nerve (GPN; Miyazaki et al., 1999; Tanaka et al., 1987). Thus, GPN on both sides was severed near the posterior lacerated foramen in 6 of 12 rats to exclude pharynx-derived reflex. A polyethylene catheter (PE50, Becton Dickinson), connected to a BP transducer (MLT0699, AD Instruments), was inserted into the left femoral artery to record the arterial pressure signal. The arterial signal detected by the BP transducer was transmitted to an amplifier for blood pressure (BP amplifier; FE117, AD Instruments). After cannulation, subcutaneous needle electrodes were attached for electrocardiography. The electrodes were set for a bipolar limb lead II and connected to a bioamplifier (MEG-5100, Nihon Koden). A polyethylene cannula was

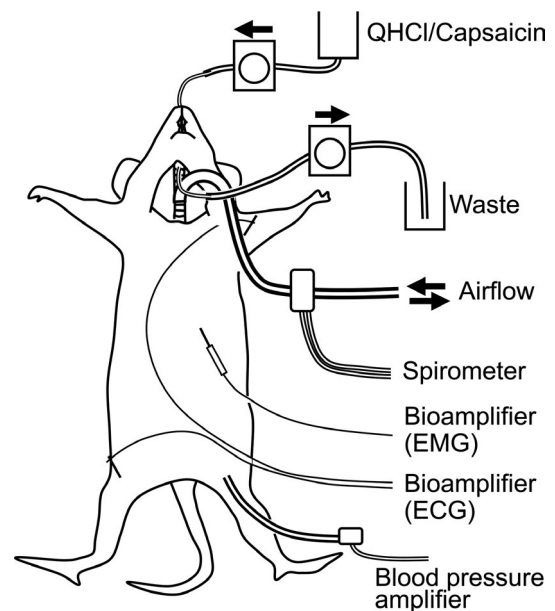


FIGURE 1 Schematic drawing of physiological experiments. Details are described in the Section 2

then inserted into the trachea to secure tracheal breathing. The cannula was connected to a respiratory flow head (MLA1L, AD Instruments) attached to a spirometer (FE141, AD Instruments) to detect airflow

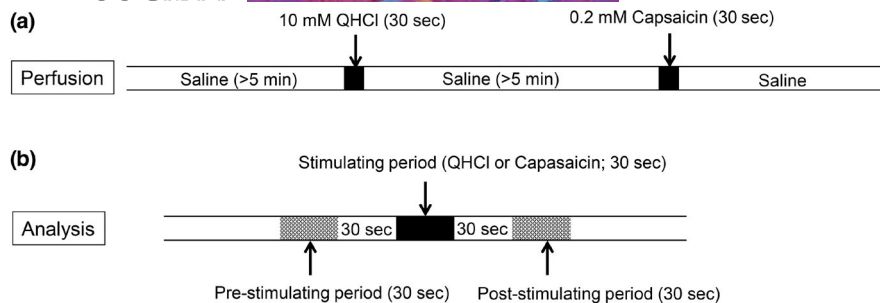


FIGURE 2 Time course of the electrophysiological experiment. (a) Time course of perfusion. (b) Analysis at three time points (arrows). Details are described in the Section 2

changes associated with respiration. A concentric electrode (NM-320T, Nihon Koden) was set to the diaphragm from the right intercostal space and connected to a bioamplifier (MEG-5100, Nihon Koden) to record electromyograms. Regarding the stimulation, tip of cannula (PE50) was inserted into the nostril 1–2 mm in length to set up solution inlet in the nasal vestibule. However, another cannula (PE50) was inserted from a tracheal incision to reach the intrapharyngeal opening as outlet. Physiological saline or stimulant solutions were continuously infused from the inlet for 30 s at 1 ml/min by a pump (Masterflex 77120-42, Cole-Parmer). In the outlet, fluid was aspirated by another pump. An inline-heater (SF-28/TC-324C Warner Instrument) was settled in the infusion line to warm fluid at 37°C. The BP amplifier, bioamplifiers, and spirometer were connected to an analog-to-digital converter (PowerLab, PL3504, AD Instruments), and respiratory flow changes and an electromyogram of the diaphragm were recorded on a computer using LabChart 7 (AD Instruments). Time-dependent changes in respiratory frequencies, heart rate, and mean blood pressure were calculated using the same software.

The time course of the experiment is shown in Figure 2. At the beginning of the experiment, animals developed apnea and recovered within 2 min. Therefore, saline was infused from the inlet and maintained for at least 5 min before the experiment. Saline was then changed to QHCl solution (10 mM in saline; 179-00461, Fujifilm Wako) for 30 s, saline for 5 min, capsaicin solution (0.2 mM in saline; 07127-21, Nacal Tesque), and then saline in that order (Figure 2a). Capsaicin was used to examine reflex caused from activation of C-fiber terminals. Respiratory frequencies (cycles per min), heart rate, and mean blood pressure were analyzed during three 30-sec time points: pre-stimulation, stimulation (QHCl or capsaicin), and post-stimulation as shown in Figure 2b. Values were shown as the average \pm SE. Mean values were statistically analyzed by a one-way ANOVA. Bonferroni corrections were used as the post-hoc analysis.

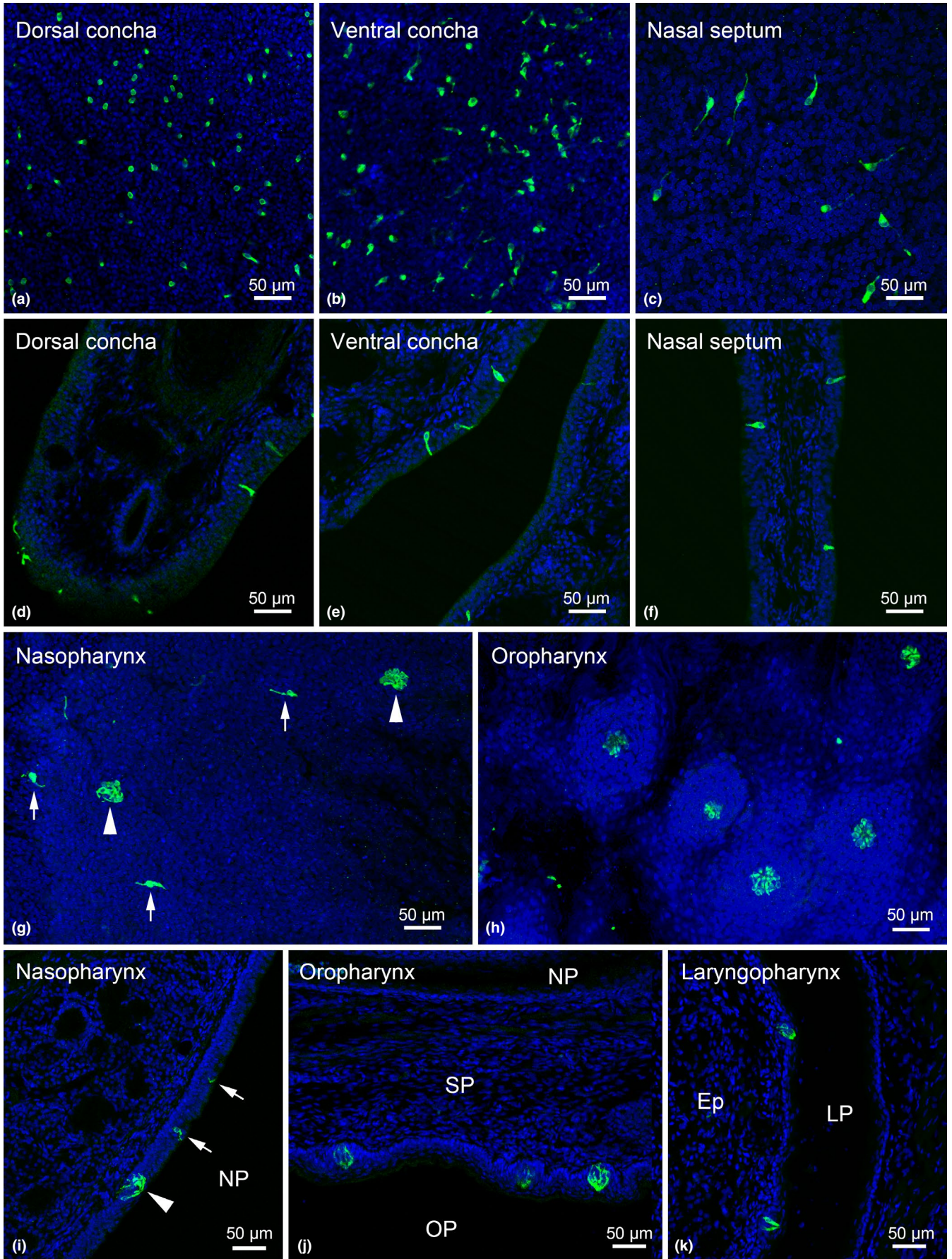
3 | RESULTS

3.1 | Morphological characteristics of solitary chemosensory cells and chemosensory cell clusters

Whole-mount preparations revealed the distribution and morphological characteristics of solitary chemosensory cells in the nasal respiratory mucosa (Figure 3a–c). Sections also showed the characteristics of the distribution and morphology of GNAT3-immunoreactive chemosensory cells (Figure 3d–f). In the dorsal concha, the majority of solitary chemosensory cells were barrel like in shape, while some were slender with lateral cytoplasmic processes (Figure 3a,d). The number of slender cells was higher in the ventral concha than in the dorsal concha (Figure 3b,e). In the nasal septum, the majority of GNAT3-immunoreactive cells were slender with elongated thick lateral cytoplasmic processes (Figure 3c,f). The density of GNAT3-immunoreactive chemosensory cells was higher in the cranial region near the nostril than in the caudal region in both the nasal concha and septum. Chemosensory clusters were not detected in the nasal cavity.

The pharynx of the rat was divided into three parts: the nasopharynx, oropharynx, and laryngopharynx. In the nasopharynx, the part from the choana to intrapharyngeal opening, solitary chemosensory cells and chemosensory cell clusters were observed in the lateral sides of the pharyngeal cavity near the intrapharyngeal opening (Figure 3g,i). The majority of chemosensory cells in the nasopharynx were slender in shape with complex processes. Clusters of chemosensory cells consisted of a relatively small number of cells. In the oropharynx, which is the part of the fauces to the palatolingual arch, solitary chemosensory cells were not detected, and well-developed taste bud-like clusters of chemosensory cells were distributed in the soft palate (Figure 3h,j). In the laryngopharynx, the part from the palatopharyngeal arch to the pharyngoesophageal boundary, no chemosensory cells were observed in the lateral wall,

FIGURE 3 Distribution of GNAT3-immunoreactive cells in the nasal mucosa (a–f) and pharyngeal mucosa (g–k). The distribution and cell shape of solitary chemosensory cells and chemosensory cell clusters are shown in whole-mount preparations (a–c, g, h) and cryostat sections (d–f, i–k). In the nasal mucosa, solitary chemosensory cells that were barrel-like or slender in shape were distributed in the dorsal concha (a, d), ventral concha (b, e), and nasal septum (c, f), whereas chemosensory clusters were absent. Solitary chemosensory cells (arrows) and clusters (arrowheads) were both distributed in the nasopharynx (g, i). Chemosensory cell clusters were distributed in the oro- and laryngopharynx, whereas solitary chemosensory cells were not (h, j, k). Nuclei are labeled by DAPI (blue)



and chemosensory cell clusters were distributed in the lateral side of the larynx (Figure 3k).

3.2 | Morphology of chemosensory cells

The morphology of solitary chemosensory cells was variform. Barrel-like cells that were mainly distributed in the ventral concha consisted of a rounded perinuclear region and thick apical process (Figure 4a). The apical process reached the lumen of the nasal mucosa. Slender cells in the nasal cavity consisted of a perinuclear region, one apical process, and long thick lateral cytoplasmic processes (Figure 4b,c). The apical process faced the cavity, and the lateral processes were elongated within the epithelial layer. In the nasopharynx, the shape of cells appeared to be more complex and diverse (Figure 4d–f). They showed a perinuclear region, a short apical process facing the lumen, and variform lateral cytoplasmic processes. The lateral processes varied in thickness; thick, slender, and filamentous in shape and ranging in number between 2 and 7. In Figure 4e, seven filamentous processes were arranged. In some cases, two processes were fused to each other, as shown in Figure 4d,f.

Chemosensory cell clusters were widely distributed in the pharyngeal cavity (Figure 5a–c). GNAT3-immunoreactive cells gathered with SNAP25-immunoreactive cells and/or nerve fibers within the epithelial layer. In the nasopharynx, pleomorphic cells gathered with SNAP25-immunoreactive cells in the transitional epithelium to form chemosensory cell clusters (Figure 5a). Chemosensory clusters in the oropharynx were larger in size and scattered in the stratified squamous epithelium of the soft palate. Within clusters in the soft palate, slender GNAT3-immunoreactive chemosensory cells were arranged with SNAP25-immunoreactive cells (Figure 5b). The clusters of chemosensory cells in the laryngopharynx were similar to those in the soft palate, but were smaller in size (Figure 5c). Whole-mount preparations showed the 3D architecture of chemosensory clusters (Figure 5d,e). In Figure 5d, two GNAT3-immunoreactive cells were closely arranged in the epithelial layer of the nasopharynx, whereas apical processes did not gather at one point. One of the chemosensory cells had a flattened process wrapping around cells without GNAT3 immunoreactivity. The nasopharyngeal chemosensory cell clusters shown in Figure 5e contained 13 GNAT3-immunoreactive cells and 3 SNAP25-immunoreactive cells. The shape of chemosensory cells in the cluster varied. The apical processes of most of the cells faced the luminal surface at one point. On the other hand, branched processes were shown at the basal aspect. Some cells were elongated around the cluster.

3.3 | Immunohistochemical localization of taste-signaling molecules

GNAT3-immunoreactive cells were also immunoreactive for PLC β 2 and IP3R3 in the nasal cavity and pharynx (Figure 6). Triple immunolabeling confirmed that GNAT3-immunoreactive cells were immunoreactive for both PLC β 2 and IP3R3 (Figure 6g–i). Immunoreactivity

for PLC β 2 and IP3R3 was observed in both solitary chemosensory cells and chemosensory cell clusters.

3.4 | Nerve endings in solitary chemosensory cells and chemosensory cell clusters

In the nasal cavity and nasopharynx, GNAT3-immunoreactive solitary chemosensory cells were in close contact with thin intraepithelial free nerve endings with SP or CGRP immunoreactivity (Figure 7a–d). Whole-mount preparations revealed that punctate-free SP- and CGRP-immunoreactive nerve endings were in contact with GNAT3-immunoreactive solitary chemosensory cells at the perinuclear region, apical cytoplasmic process, and elongated long processes. As shown in Figure 7b, CGRP-immunoreactive nerves were in contact with a long lateral cytoplasmic process. In chemosensory cell clusters in the naso-, oro-, and laryngopharynx, varicosities of SP- and CGRP-immunoreactive nerve endings were sparsely diffused between GNAT3-immunoreactive cells and nerve fibers accumulated beneath and around the clusters (Figure 7e–g). Bassoon immunoreactivity was observed on the SP- or CGRP-immunoreactive varicosities, but not on the GNAT3-immunoreactive cells (Figure 8).

In the nasopharynx, P2X3-immunoreactive nerve endings tightly attached to GNAT3-immunoreactive cells in addition to nerve endings with SP or CGRP immunoreactivity. In the nasal mucosa, P2X3-immunoreactive nerve endings were not observed either in the whole-mount preparation from three rats and cryostat sections nasal mucosa from other three rats (Figure 9). P2X3-immunoreactive nerve endings were closely attached to the perinuclear region and elongated lateral processes of GNAT3-immunoreactive cells (Figure 9a,b). In chemosensory clusters in the pharynx, the thick arborizations of P2X3-immunoreactive nerve endings deeply intruded into the clusters and attached to GNAT3-immunoreactive cells (Figure 9c).

3.5 | Reflex evoked by QHCl and capsaicin in the nasal cavity and pharynx

In a representative case of intact rats (Figure 10a, left panel), the perfusion of QHCl (10 mM, 30 s) into the nasopharyngeal cavity induced the depression of tracheal breathing and decreased electromyogram activity in the diaphragm. Heart rate and mean blood pressure decreased and increased, respectively. As shown in the right panel of Figure 10a, the perfusion of capsaicin altered respiratory frequency, heart rate, and mean blood pressure. In a representative case of GPN (IX)-severed rats, these parameters remained unchanged during the perfusion of QHCl, but showed similar changes to those in intact rats with the perfusion of capsaicin (Figure 10b).

Changes in autonomic parameters varied in individuals (Figure 11), and the results obtained are shown in Table 4. In 2 of 6 intact rats, apnea was induced by the perfusion of QHCl (Figure 11a). Respiratory frequency was significantly higher in the

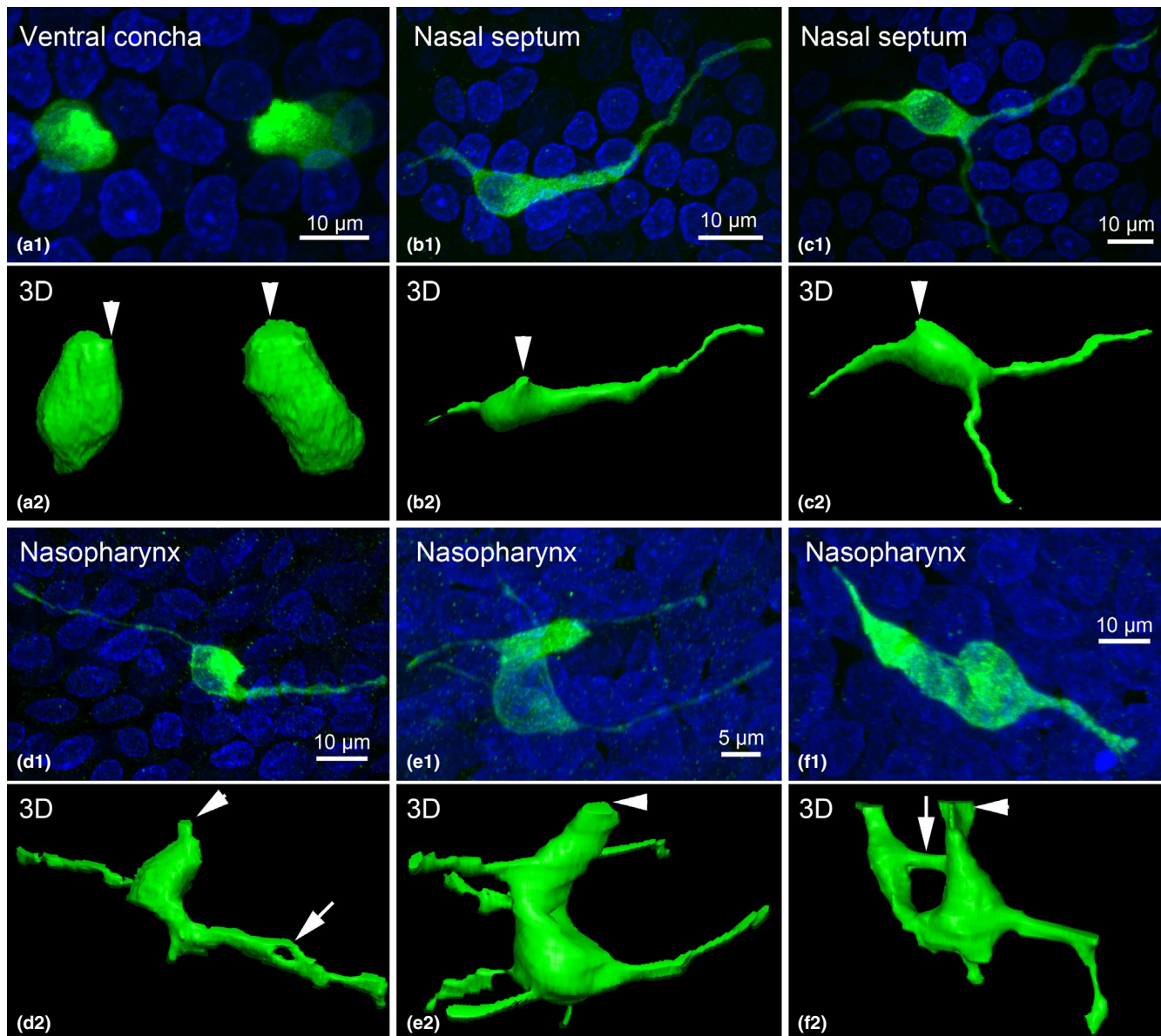


FIGURE 4 Morphology of GNAT3-immunoreactive cells (green) in whole-mount preparations of the nasal respiratory mucosa (a–c) and nasopharynx (d–f). Nuclei are labeled by DAPI (blue). Panels numbered 1 (a-1 to f-1) are projection views of z-stack images. Panels numbered 2 (a-2 to f-2) are three-dimensional views reconstructed from binary images of panels numbered 1. Arrowheads in each second panel indicate the part of the apical process facing the nasal or pharyngeal cavity. (a) Barrel-like cells in the ventral concha. (b, c) A slender cell with two or three thick lateral processes in the nasal septum. (d–f) Complex-shaped solitary chemosensory cells in the nasopharynx. Arrows in d and f are fused cytoplasmic processes. In panel e, seven filamentous processes are arranged in the chemosensory cell

pre-perfusion period ($p < 0.05$) in intact rats (Table 4). Even in IX-severed rats, ventilatory depression was observed in 2 of 6 rats following the perfusion of QHCI (Figure 11a). Heart rate was reduced by QHCI to less than 90% that in the pre-perfusion period in 2 of 6 rats (Figure 11b). Mean blood pressure was increased by QHCI up to 110% in 2 and 1 intact and IX-severed rats, respectively (Figure 11c). Mean blood pressure in the QHCI perfusion period was significantly different from that in the pre-perfusion period in IX-severed rats ($p < 0.05$; Table 4). When capsaicin solution was perfused into the nasopharyngeal cavity, apnea was observed in

2 and 4 intact and IX-severed rats, respectively (Figure 11d). In both groups, respiratory frequency in the capsaicin perfusion period was significantly different from those in the pre- and post-perfusion periods ($p < 0.01$; Table 4). Heart rate was reduced by capsaicin to $<90\%$ in 2 and 3 intact and IX-severed rats, respectively (Figure 11f). Blood pressure was increased by up to 110% from that in the pre-perfusion period by capsaicin in 3 and 5 intact and IX-severed rats, respectively (Figure 11e). In intact rats, mean blood pressure in the capsaicin perfusion period significantly differed from that in the pre-perfusion period ($p < 0.05$).

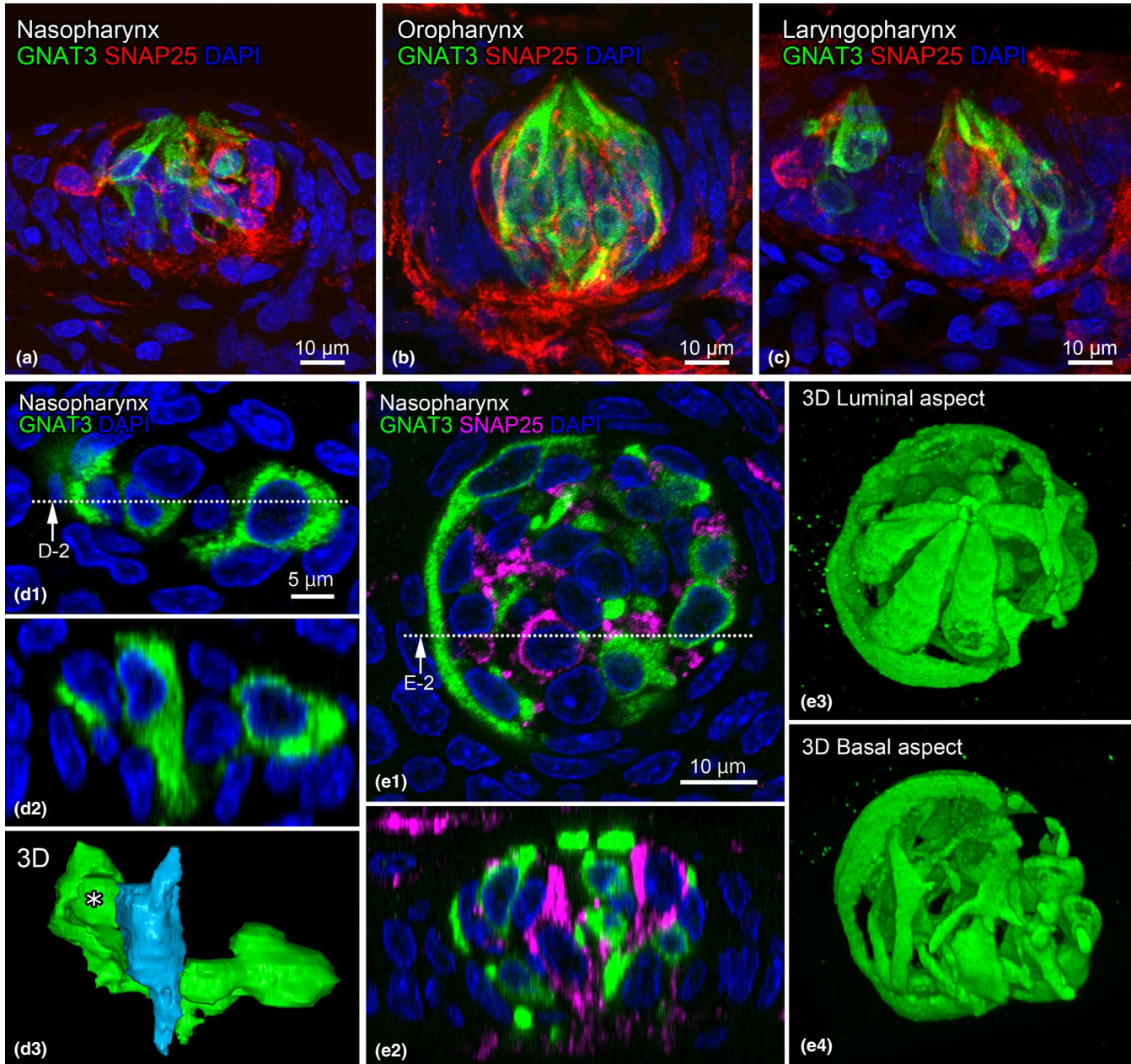


FIGURE 5 Morphology of clusters of chemosensory cells in the pharyngeal mucosa. (a–c) Chemosensory clusters containing GNAT3-immunoreactive cells (*green*) in the naso- (a), oro- (b), and laryngopharynx (c) in cryostat sections. SNAP25-immunoreactive cells and/or nerve fibers (*red*) are shown in the clusters. (d, e) Chemosensory cell clusters in whole-mount preparations of the nasopharynx. Clusters in panels d and e contained 2 and 13 GNAT3-immunoreactive cells (*green*), respectively. The cluster in panel e contained 3 SNAP25-immunoreactive cells (*magenta*). d-1 and e1 are horizontal sections of chemosensory cell clusters selected from z-stack series, and d-2 and e-2 are sectional views at the dotted line indicated in d-1 and d2. d3 shows three-dimensional reconstruction views from a binary image of panel d-1 of a slender cell (*light blue*) and cells (*green*) with a flattened cytoplasmic process wrapping around the epithelial cell (asterisk). e-4 and e-5 are apical and basal views, respectively, of a cluster composed of alpha blending. Cellular nuclei are counterstained with DAPI in panels a–c, d-1, d-2, e-1, and e-2 (*blue*)

4 | DISCUSSION

The present results showed the morphology, distribution, and innervation of solitary chemosensory cells and chemosensory cell clusters in the nasal and pharyngeal mucosae using whole-mount preparations with immunofluorescence for GNAT3. Furthermore, nasopharyngeal reflexes that may have been induced by the activation of chemosensory cells were recorded.

4.1 | Distribution and morphology of solitary chemosensory cells

In the nasal cavity, solitary chemosensory cells were widely distributed in the nasal mucosa (Finger et al., 2003; Lin et al., 2008; Tizzano et al., 2010). The findings of immunohistochemistry for α -gustducin (synonym of GNAT3) revealed that nasal solitary chemosensory cells were densely distributed in the anterior part of the turbinate

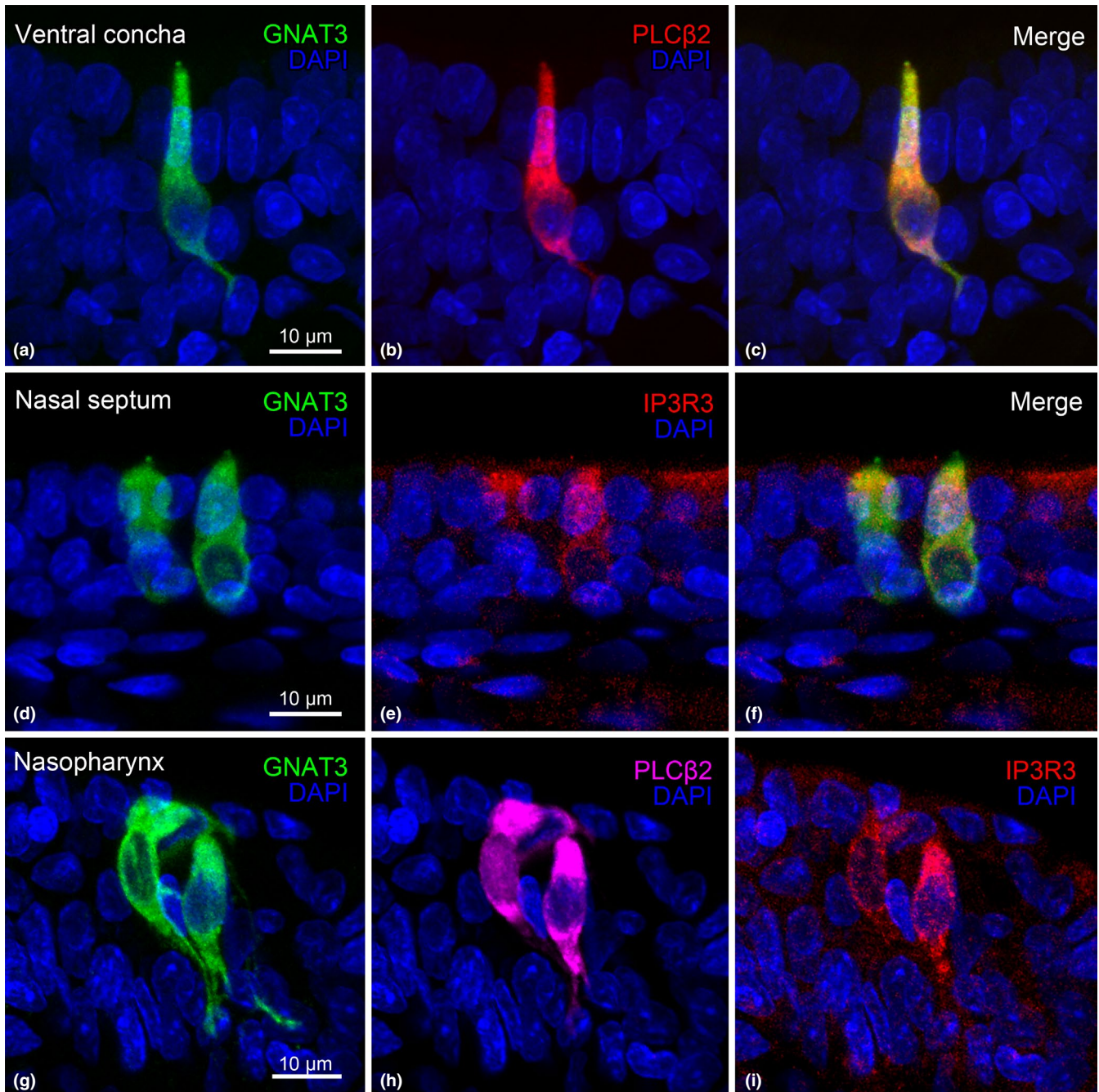


FIGURE 6 Double or triple immunofluorescence for GNAT3 with PLC β 2 and/or IP3R3 in the nasopharyngeal cavity. (a–c) A GNAT3-immunoreactive solitary chemosensory cell (*green*) in the ventral concha is also immunoreactive for PLC β 2 (*red*). (d–f) A GNAT3-immunoreactive solitary chemosensory cell (*green*) in the nasal septum is also immunoreactive for IP3R3 (*red*). (g–i) GNAT3-immunoreactive chemosensory cells (*green*) in a small cluster in the nasopharynx are also immunoreactive for both PLC β 2 (*magenta*) and IP3R3 (*red*). Nuclei are labeled by DAPI (*blue*)

facing air passage in the rat (Finger et al., 2003). Furthermore, the distribution of TRPM5-expressing cells was similar to that of α -gustducin-immunoreactive cells (Gulbransen, Clapp, et al., 2008; Lin et al., 2008). The present study confirmed the distribution of chemosensory cells in the anterior part of the nasal cavity. In addition to the anterior part of the nasal mucosa facing air passage, the present study revealed the distribution of solitary chemosensory cells in the anterior part of the pharyngeal cavity with chemosensory

cell clusters. The distribution pattern of chemosensory cells in the nasopharynx appeared to be similar to that of the 'edge of the epiglottis' or 'tip of the corniculate process' of the larynx as previously reported (Masuda et al., 2019). These results indicate that nasal and pharyngeal solitary chemosensory cells monitor irritant chemical substances entering and exiting the nasal cavity, respectively.

Previous studies reported that nasal chemosensory cells were spindle shaped (Finger et al., 2003). In the present study, a

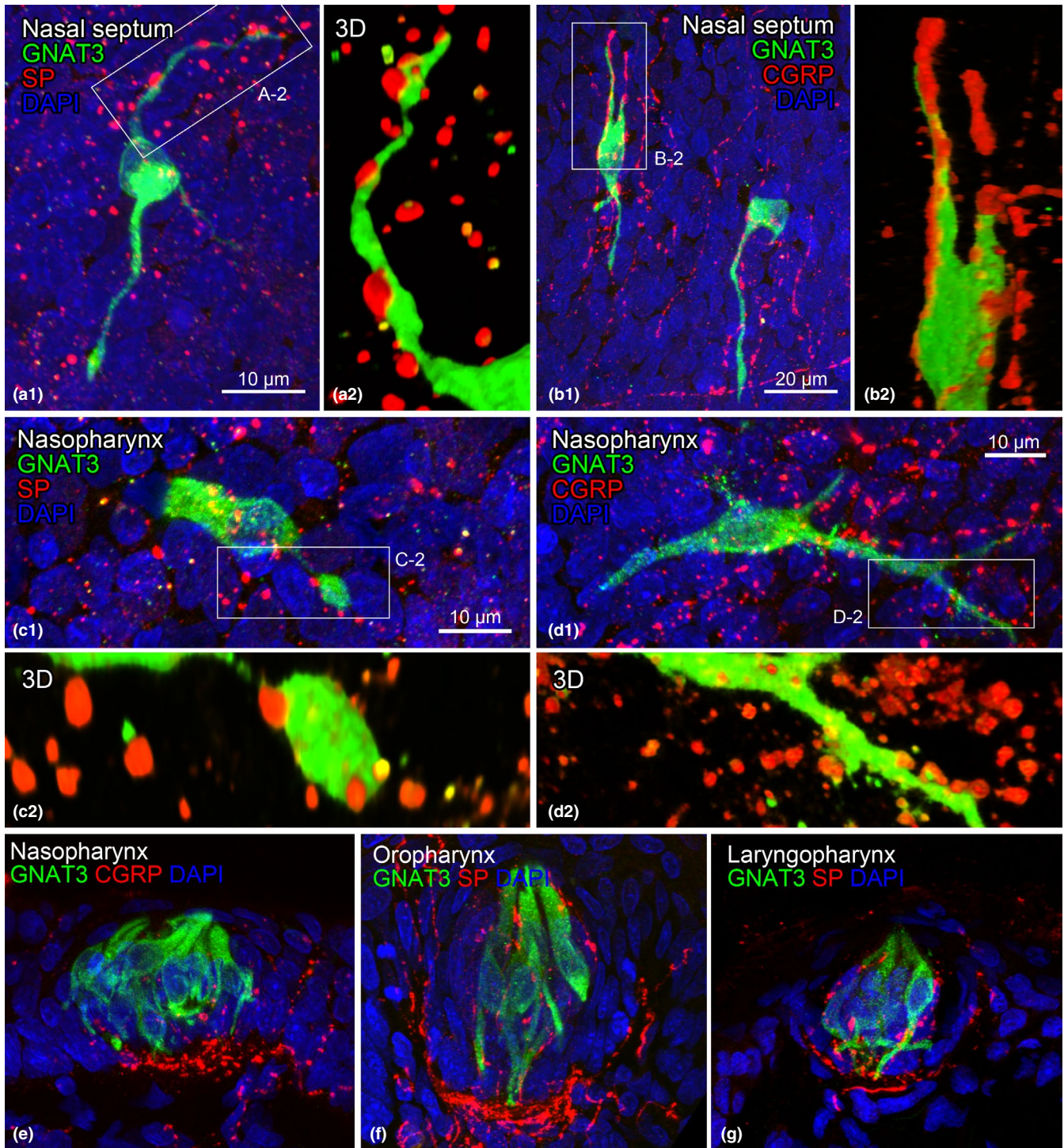


FIGURE 7 Double immunofluorescence for GNAT3 (green) with SP (red; A, C, F, G) or CGRP (red; b, d, e) in solitary chemosensory cells (a–d) and chemosensory cell clusters (e–g) in the nasopharyngeal cavity. Panels numbered 1 (a-1 to d-1) are the luminal projection view of z-stack series of whole-mount preparations. Panels numbered 2 (a-2 to d-2) are a three-dimensional reconstruction view of panels numbered 1 composed by alpha blending. Panels e–g are z-stack projection views of cryostat sections. Nuclei are labeled by DAPI in a-1, b-1, c-1, d-1, and e-g (blue). (a, b) Slender solitary chemosensory cells in the nasal septum are attached to free nerve endings with immunoreactivity for SP (a) and CGRP (b). (c, d) Complex-shaped solitary chemosensory cells in the nasopharynx are attached to varicosities immunoreactive for SP (c) and CGRP (d). (e–g) A few SP- or CGRP-immunoreactive varicosities are distributed within chemosensory cell clusters in the naso- (e), oro- (f), and laryngopharynx (g)

number of complex-shaped solitary chemosensory cells were observed in whole-mount preparations of the nasal and pharyngeal mucosae. Common characteristics of GNAT3-immunoreactive

cells in the nasal and pharyngeal mucosae were the apical cytoplasmic process reaching the lumen of the airway cavity and variform lateral processes within the epithelial layer, which were

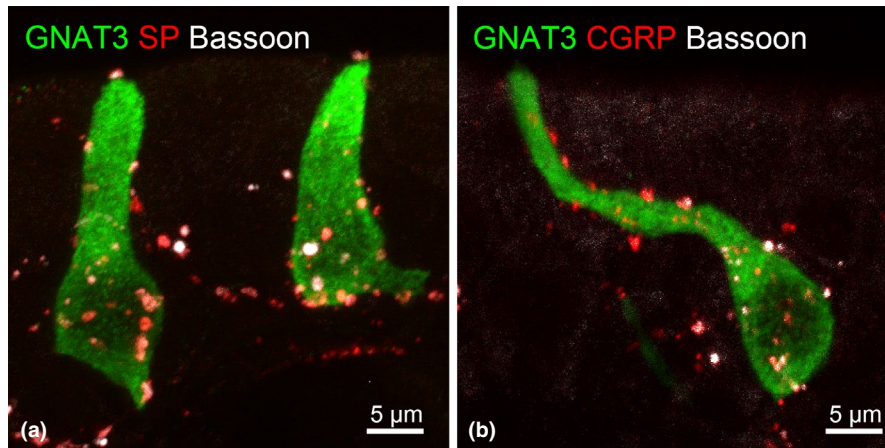


FIGURE 8 Triple immunofluorescence for GNAT3-immunoreactive solitary chemosensory cells (green) and SP- or CGRP-immunoreactive nerve endings (red) with bassoon immunoreactivity (white) in the nasal septum. Bassoon immunoreactive puncta are observed on the SP- or CGRP-immunoreactive nerve endings

similar to laryngeal solitary chemosensory cells (Masuda et al., 2019). Immunoreactivities for PLC β 2 and IP3R3 were also detected in chemosensory cells in the nasopharyngeal cavity, similar to the larynx and trachea (Lin et al., 2008). Previous studies showed immunoreactivity for gustducin in some taste cells in the circumvallate papillae and soft palate of the rat (Clapp et al., 2001; Miura et al., 2007), and nasal chemosensory cells have been suggested to express taste signaling molecules in different patterns. In tracheal 'brush cells' expressing choline acetyltransferase with GNAT3, PLC β 2, and TRPM5, acetylcholine was released by a denatonium stimulation for ciliary motility in ciliated cells and autocrine regulation (Hollenhorst et al., 2020). Furthermore, it has been reported that intracellular Ca²⁺ concentration in the nasal solitary chemosensory cells were increased by acyl-homoserine lactone produced by gram-negative bacteria as quorum-sensing signals (Tizzano et al., 2010). The activation of solitary chemosensory cells propagates to surrounding respiratory epithelial cells to secrete antibacterial peptides such as β -defensin 2 in sinonasal mucosa (Lee et al., 2014). Furthermore, the chemosensory cells also produce acetylcholine to activate motility of cilia of surrounding ciliated cells via muscarinic M3 receptors (Perniss et al., 2020). Widespread intraepithelial cytoplasmic processes in nasal and pharyngeal solitary chemosensory cells may effectively regulate other epithelial cells to protect mucosal infection of bacteria. On the other hand, it has been also reported the ciliated cells in the respiratory mucosa expressed T2R taste receptors, and activated by bitter substances such as denatonium, thujone, and quinine (Shah et al., 2009). Furthermore, acyl-homoserine lactone directly activated T2R38 in the ciliated cells to increase ciliary beats and to produce nitric oxide for killing bacteria (Lee et al., 2012). Therefore, mucosal immunity of nasopharyngeal mucosa by the solitary chemosensory cells would maintain in cooperation with the surrounding ciliated cells.

4.2 | Distribution and morphology of chemosensory cell clusters

A large number of solitary chemosensory cell clusters were observed in the pharynx, whereas there were few solitary chemosensory cells. The distribution and morphology of pharyngeal 'taste buds' have been extensively examined (Klein & Schroeder, 1979; Sekerková et al., 2005; Travers & Nicklas, 1990). The morphology of chemosensory cell clusters was smaller in the nasopharynx than in the oropharynx. Chemosensory cell clusters in the lateral wall of the laryngopharynx appeared to be similar to those in the nasopharynx and larynx. Since the epiglottis projected into the nasopharyngeal cavity, at least in cryostat sections, chemosensory cell clusters in the laryngopharynx appear to detect chemical substances at the entrance of the lower airway with clusters in the nasopharynx and larynx. Clusters in the nasopharynx and laryngopharynx consist of pleomorphic GNAT3-immunoreactive cells and appear to be similar to those in the laryngeal mucosa (Masuda et al., 2019). Histologically, the oropharynx and laryngopharynx are lined with thick and thin stratified squamous epithelia, respectively, while the nasopharynx is lined with a transitional epithelium. Thus, morphological differences in chemosensory clusters may be related to the epithelial type and its thickness. In the laryngeal mucosa, chemosensory cell clusters were distributed with solitary chemosensory cells, and consisted of variform GNAT3-immunoreactive cells and spindle SNAP25-immunoreactive cells (Masuda et al., 2019). Similar to chemosensory cell clusters in the larynx, SNAP25-immunoreactive cells were present in addition to GNAT3-immunoreactive chemosensory cells, the clusters immunoreactive for GNAT3 in pharyngeal chemosensory cell clusters. In the oral taste buds, SNAP25 immunoreactivity was observed in type III cells responsible for sour perception (Yang et al., 2000). In the oropharynx, for example, the soft palate, chemosensory cell clusters were larger and consisted of numerous spindle

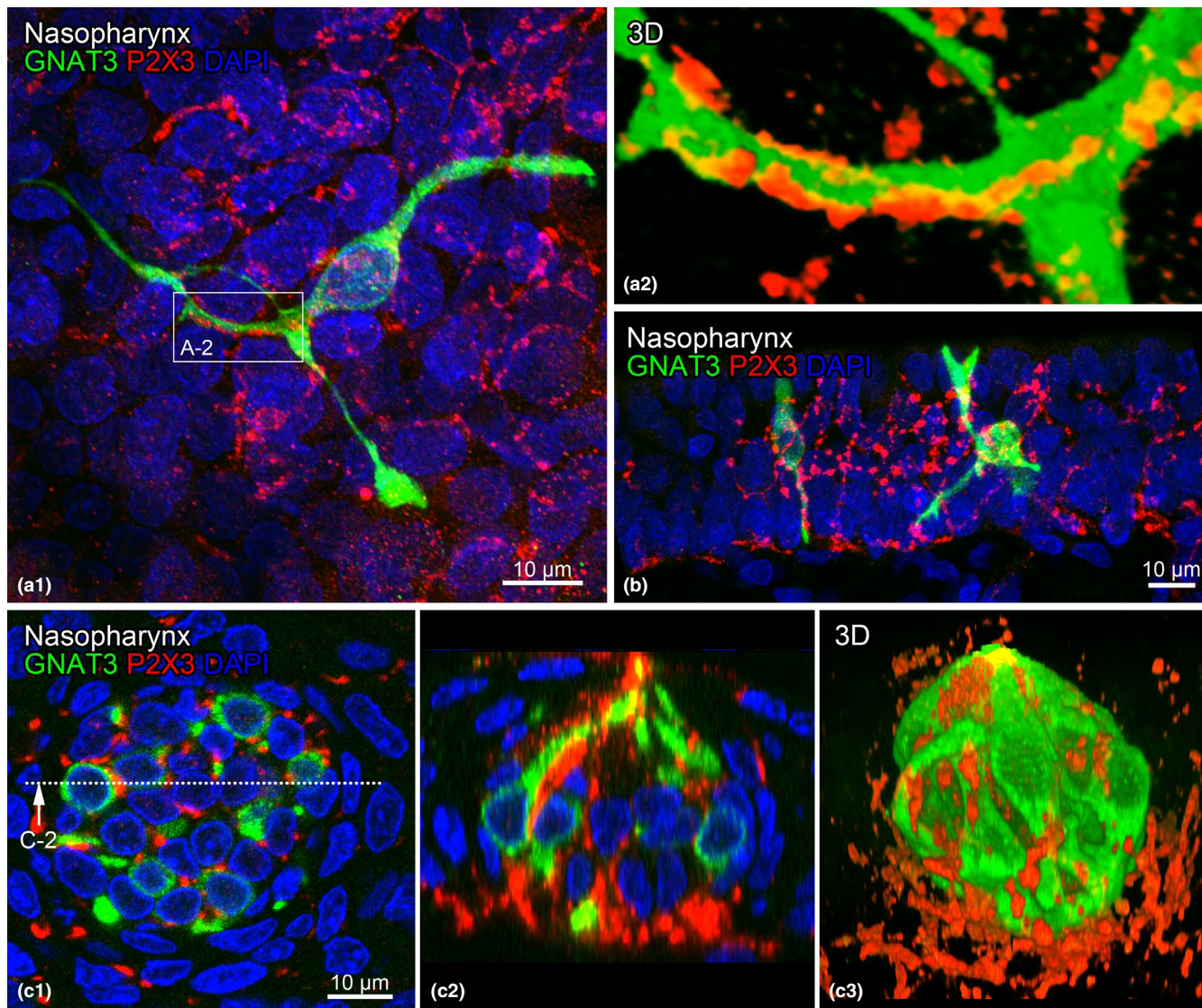


FIGURE 9 P2X3-immunoreactive nerve endings around GNAT3-immunoreactive solitary chemosensory cells (a, b) and chemosensory cells in clusters (c) in the nasopharynx. (a) Projection view (a-1) and three-dimensional reconstruction view (a-2) of P2X3-immunoreactive nerve endings (red) around GNAT-immunoreactive cells with lateral processes (green). P2X3-immunoreactive nerve endings in contact with GNAT3-immunoreactive cells. (b) GNAT3-immunoreactive cells and associated P2X3-immunoreactive nerve endings shown in the cryostat section. (c) Panel c-1 is a horizontal section of chemosensory cell clusters selected from z-stack series, c-2 is a sectional view at the dotted line indicated in c-1, and c-3 is a three-dimensional reconstruction view. Arborized P2X3-immunoreactive nerve endings (red) are in close contact with GNAT3-immunoreactive chemosensory cells (green). Nuclei are labeled by DAPI in a-1, b, c-1, and c-2 (blue)

cells. They were similar to the oral taste buds in the lingual papillae, and may play a role in taste sensing at the caudal part of the oropharyngeal cavity.

4.3 | Innervation of solitary chemosensory cells and chemosensory cell clusters

In the present study, P2X3-immunoreactive nerve endings were not observed around nasal solitary chemosensory cells, whereas numerous nerve fibers immunoreactive for SP and CGRP were attached to cells, as previously reported (Finger et al., 2003; Tizzano et al.,

2010). In the present study, double immunofluorescence indicates varicosities immunoreactive to SP and CGRP contained bassoon, one of the scaffold proteins of presynaptic active zone. In the striatum, dopamine is released from active zone-like sites with bassoon, RIM and ELKS in the varicosities (Liu et al., 2018). Although electron microscopic study showed the presence of afferent synapse in the nasal solitary chemosensory cells (Finger et al., 2003), bassoon immunoreactivity in the varicosities seems that the SP- and CGRP-immunoreactive nerve endings may be presynaptic site. Thus, SP- or CGRP-immunoreactive nerve endings around the solitary chemosensory cells may efferently modulate the chemosensory cells by secreting neuropeptides, SP or CGRP. On the other hand,

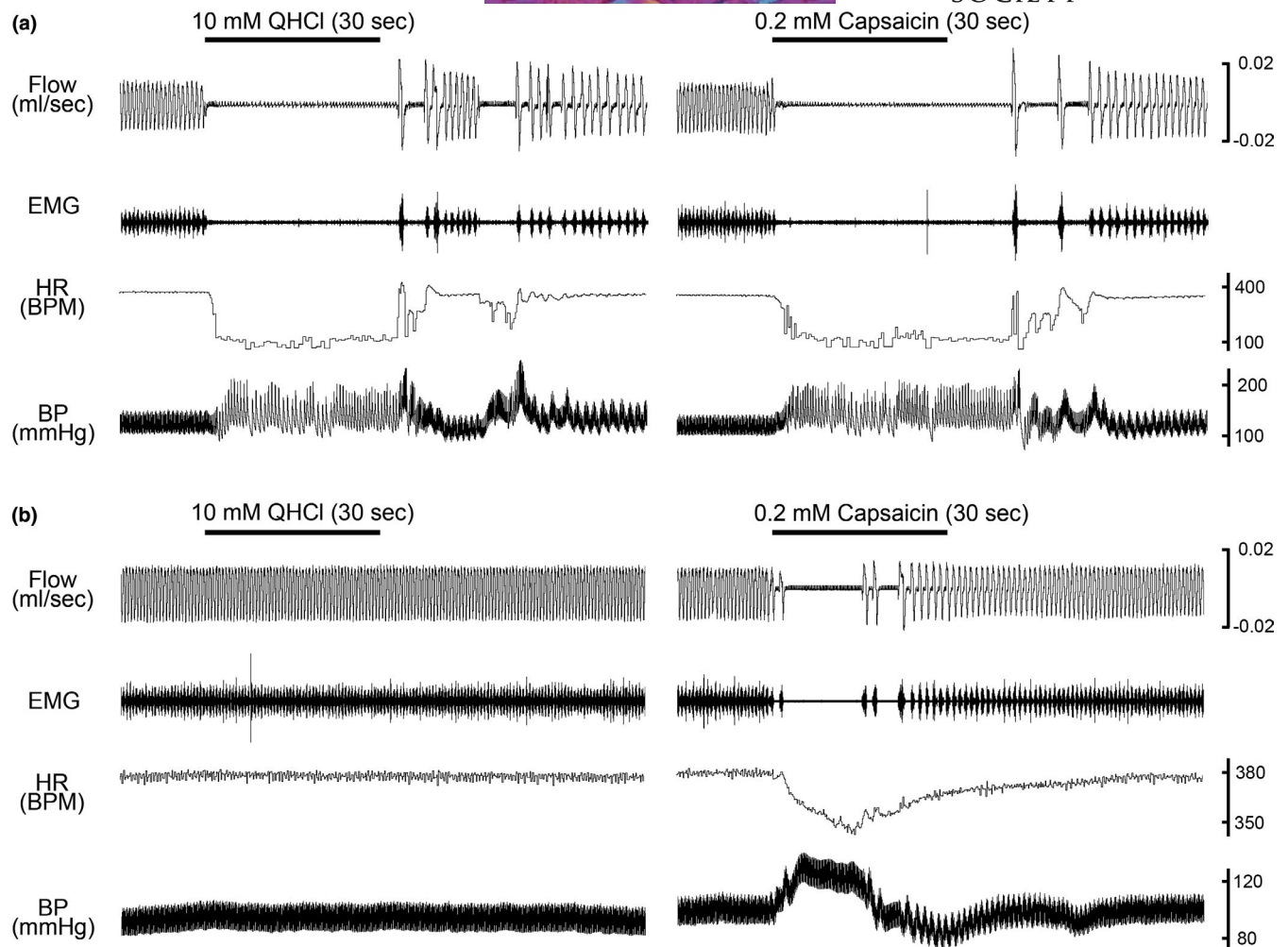


FIGURE 10 Representative traces of changes in respiratory flow (Flow), electromyographic activity of the diaphragm (EMG), heart rate (HR), and blood pressure (BF) when 10 mM QHCl and 0.2 mM capsaicin were applied to the nasopharyngeal cavity of intact rats (a) and rats with severed bilateral glossopharyngeal nerves (b). (a) The perfusion of both QHCl or capsaicin into the nasopharyngeal cavity of intact rats induced apnea, decreased EMG, and increased BP. (b) In rats with severed bilateral glossopharyngeal and superior laryngeal nerves, cardiorespiratory changes were diminished when QHCl was perfused. The perfusion of capsaicin induced similar effects to those in intact rats

TABLE 4 Changes in respiratory frequency, heart rate, and mean blood pressure following the infusion of QHCl and capsaicin into the nasal cavity and pharynx

	Respiratory frequency (Cycles/min \pm SE)		Heart rate (Beats/min \pm SE)		Mean blood pressure (mmHg \pm SE)	
	Intact	IX severed	Intact	IX severed	Intact	IX severed
Pre-stimulating period	96.0 \pm 6.6	106.0 \pm 2.9	356.6 \pm 18.7	398.0 \pm 15.7	121.4 \pm 2.1	116.5 \pm 2.5
10 mM QHCl	57.0 \pm 14.5 ^b	96.0 \pm 5.9	305.0 \pm 42.2	397.5 \pm 15.0	129.2 \pm 3.8	121.1 \pm 2.7 ^b
Post-stimulating period	88.9 \pm 6.8	106.2 \pm 2.7	348.1 \pm 6.9	395.6 \pm 15.2	122.3 \pm 1.9	117.6 \pm 2.7
Pre-stimulating period	88.2 \pm 5.8	104.6 \pm 2.3	328.4 \pm 23.4	387.6 \pm 18.3	120.7 \pm 4.0	116.6 \pm 5.6
0.2 mM Capsaicin	38.9 \pm 12.1 ^a	31.0 \pm 9.9 ^a	271.3 \pm 42.5	330.1 \pm 33.3	132.2 \pm 5.8 ^a	141.9 \pm 9.3
Post-stimulating period	74.0 \pm 6.9	91.9 \pm 2.9	323.3 \pm 23.8	387.3 \pm 14.9	124.3 \pm 4.9	119.8 \pm 5.7

Intact, control animals ($n = 6$); IX severed, animals with a severed bilateral glossopharyngeal nerve ($n = 6$).

^a $p \leq 0.01$ versus pre- and post-stimulating periods.

^b $p \leq 0.05$ versus the pre-stimulating period; One-way ANOVA and Bonferroni test.

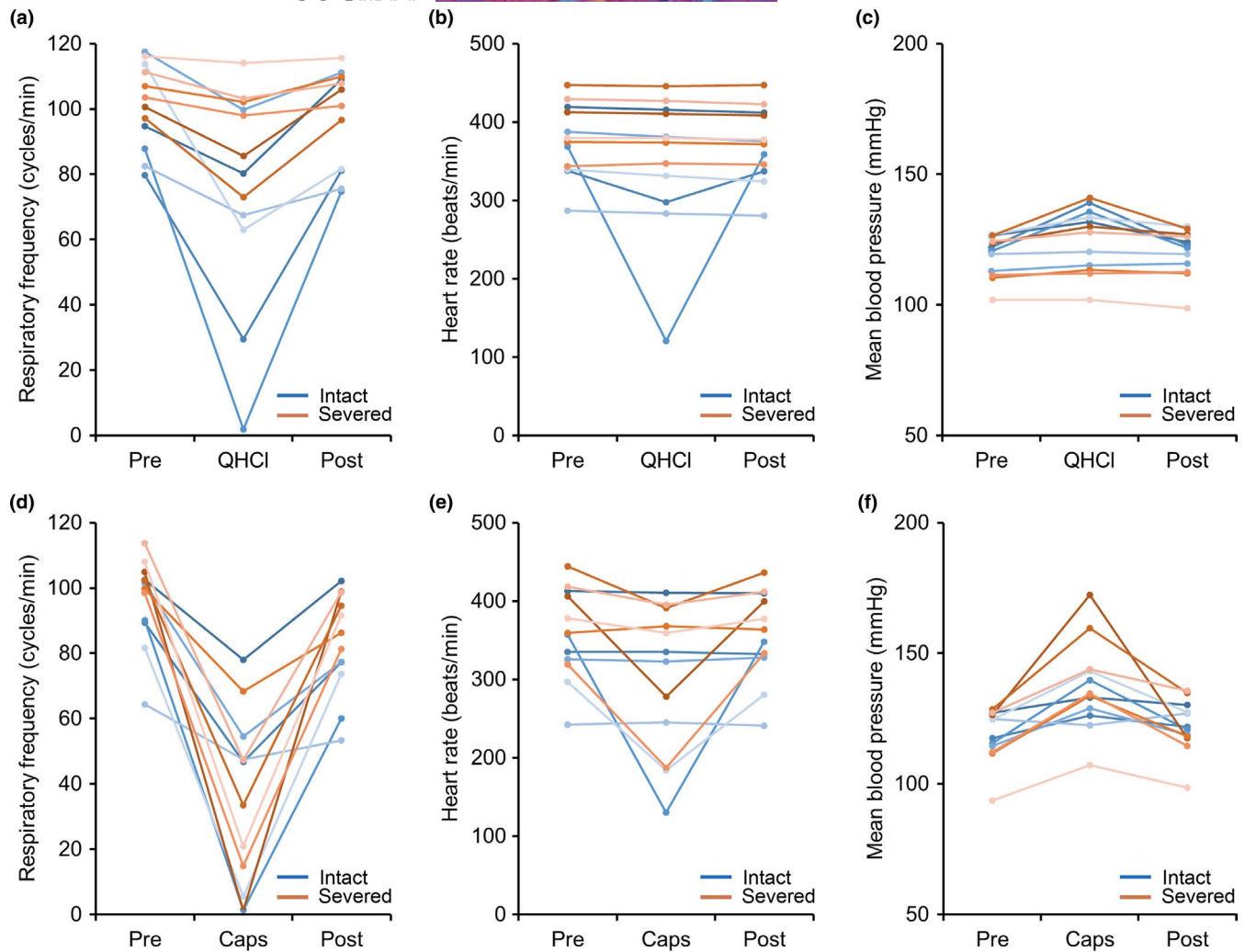


FIGURE 11 Changes in respiratory frequency (a, d), heart rate (b, e), and mean blood pressure (c, f) when QHCl (10 mM; a–c) and capsaicin (0.2 mM; d–f) were perfused into the nasopharyngeal cavity. Lines colored blue and orange are intact rats ($n = 6$) and rats with severed bilateral glossopharyngeal nerves ($n = 6$), respectively

pharyngeal solitary chemosensory cells were closely attached to P2X3-immunoreactive nerve endings, similar to the larynx (Masuda et al., 2019; Takahashi et al., 2016). P2X3-immunoreactive nerve endings were also observed in pharyngeal chemosensory cell clusters. Previous studies suggested that sensory information generated by nasal solitary chemosensory cells was transmitted by free nerve endings (Tizzano & Finger, 2013). On the other hand, type II taste cells in taste buds containing GNAT3 released ATP to activate P2X receptors in taste fibers (see reviews, Kinnamon & Finger, 2013; Roper, 2013). Therefore, nasopharyngeal solitary chemosensory cells may transport chemical stimuli via P2X3-immunoreactive nerve endings from the pharyngeal lumen, but not from the nasal cavity. On the other hand, extracellular ATP has been shown to regulate ciliary beating and mucus secretion in the respiratory epithelium via P2X and/or P2Y receptors (Droguett et al., 2017; Hayashi et al., 2005; Winkelmann et al., 2019). Based on these findings, chemosensory cells in the nasopharyngeal mucosa may also regulate nasal epithelial cells by ATP released from the lateral cytoplasmic processes of nasal solitary chemosensory cells.

4.4 | Reflex caused by QHCl and capsaicin

The perfusion of saline containing denatonium benzoate, QHCl, or cycloheximide into the nasal cavity induced apnea in rats and mice (Finger et al., 2003; Tizzano & Finger, 2013). The present study showed that the perfusion of QHCl solution into the nasopharyngeal cavity induced a cardiorespiratory reflex to varying degrees. Therefore, the stimulation of the nasopharyngeal mucosa by QHCl may induce ventilatory depression or apnea. Furthermore, decreases in ventilatory depression after bilateral section of the GPN suggested a respiratory reflex caused from pharyngeal mucosa because GPN innervate pharyngeal mucosa but not nasal mucosa. A previous study reported that a nasopharyngeal stimulation by QHCl induced a cardiovascular reflex via the pharyngeal branch of the GPN (Hanamori & Ishiko, 1993). The present study indicated that a stimulation of the pharyngeal mucosa by QHCl evoked a respiratory reflex; however, the effects of the nasopharyngeal stimulation by QHCl on heart rate and blood pressure remain unclear. Therefore, the present results demonstrated that pharyngeal chemosensory

cells evoked a respiratory reflex to bitter stimuli and that the participation of nasal chemosensory cells was limited. We previously showed that the perfusion of QHCI into the laryngeal cavity evoked respiratory depression via the superior laryngeal nerve (Masuda et al., 2019). Numerous GNAT3-immunoreactive chemosensory cells with P2X3-immunoreactive nerve endings are distributed in the laryngeal mucosa. The activity of the GPN evoked by the QHCI solution was previously shown to be reduced in P2X2/P2X3 double knockout mice (Finger et al., 2005; Ohkuri et al., 2012). Since P2X3-immunoreactive nerve endings were attached to chemosensory cells in the pharynx, but not in the nasal cavity, these nerve endings appeared to have been effectively activated to evoke a respiratory reflex.

Physiologically, a capsaicin stimulation in the nasal cavity induced apnea in dogs and rats (Kanamaru et al., 1999; Tizzano et al., 2010). Capsaicin stimulated TRPV1 channels in C-fiber receptors containing SP and/or CGRP (for reviews, see Lee, 2009; Spina, 1996). Morphologically, C-fiber receptors appear as intraepithelial free nerve endings, and are widely distributed in the nasal and pharyngeal mucosae, as previously reported (Albegger et al., 1991; Lundblad et al., 1983; Stjärne et al., 1989; Terenghi et al., 1986; Uddman et al., 1985). Since bilateral section of the GPN did not induce marked changes in the respiratory reflex in the present study, capsaicin may directly stimulate intraepithelial free nerve endings in the nasopharyngeal mucosa. In the present study, the QHCI-induced reflex did not diminish respiratory depression after the GPN had been severed. Although the pharyngeal cavity has been identified as a receptive area for the respiratory reflex, the pharynx does not appear to be an important reflexogenic site (Horner et al., 1991), and pharyngeal chemosensory cells may evoke ventilatory depression by bitter stimuli.

AUTHOR CONTRIBUTIONS

YY designed the study. YY and TY acquired and analyzed the data. YY wrote the manuscript. TY and NN critically revised the manuscript. All authors approved the article.

DATA AVAILABILITY STATEMENT

Data are available on request from the authors.

ORCID

Yoshio Yamamoto  <https://orcid.org/0000-0002-6352-6013>

REFERENCES

- Albegger, K., Hauser-Kronberger, C.E., Saria, A., Graf, A.-H., Bernatzky, G. & Hacker, G.W. (1991) Regulatory peptides and general neuroendocrine markers in human nasal mucosa, soft palate and larynx. *Acta Oto-Laryngologica*, 111, 373–378. <https://doi.org/10.3109/00016489109137404>
- Clapp, T.R., Stone, L.M., Margolskee, R.F. & Kinnamon, S.C. (2001) Immunocytochemical evidence for co-expression of Type III IP3 receptor with signaling components of bitter taste transduction. *BMC Neuroscience*, 2, 6. <https://doi.org/10.1186/1471-2202-2-6>
- Droguett, K., Rios, M., Carreño, D.V., Navarrete, C., Fuentes, C., Villalón, M. et al. (2017) An autocrine ATP release mechanism regulates basal ciliary activity in airway epithelium. *Journal of Physiology*, 595, 4755–4767. <https://doi.org/10.1113/JP273996>
- Finger, T.E., Bottger, B., Hansen, A., Anderson, K.T., Alimohammadi, H. & Silver, W.L. (2003) Solitary chemoreceptor cells in the nasal cavity serve as sentinels of respiration. *Proceedings of the National Academy of Sciences of the United States of America*, 100, 8981–8986. <https://doi.org/10.1073/pnas.1531172100>
- Finger, T.E., Danilova, V., Barrows, J., Bartel, D.L., Vigers, A.J., Stone, L. et al. (2005) ATP signaling is crucial for communication from taste buds to gustatory nerves. *Science*, 310, 1495–1499. <https://doi.org/10.1126/science.1118435>
- Gulbransen, B.D., Clapp, T.R., Finger, T.E. & Kinnamon, S.C. (2008) Nasal solitary chemoreceptor cell responses to bitter and trigeminal stimulants *in vitro*. *Journal of Neurophysiology*, 99, 2929–2937. <https://doi.org/10.1152/jn.00066.2008>
- Gulbransen, B., Silver, W. & Finger, T.E. (2008) Solitary chemoreceptor cell survival is independent of intact trigeminal innervation. *The Journal of Comparative Neurology*, 508, 62–71. <https://doi.org/10.1002/cne.21657>
- Hanamori, T. & Ishiko, N. (1993) Cardiovascular responses to gustatory and mechanical stimulation of the nasopharynx in rats. *Brain Research*, 19, 214–222. [https://doi.org/10.1016/0006-8993\(93\)91614-X](https://doi.org/10.1016/0006-8993(93)91614-X)
- Hayashi, T., Kawakami, M., Sasaki, S., Katsumata, T., Mori, H., Yoshida, H. et al. (2005) ATP regulation of ciliary beat frequency in rat tracheal and distal airway epithelium. *Experimental Physiology*, 90, 535–544. <https://doi.org/10.1113/expphysiol.2004.028746>
- Henkin, R.I. & Christiansen, R.L. (1967) Taste localization on the tongue, palate, and pharynx of normal man. *Journal of Applied Physiology*, 22, 316–320. <https://doi.org/10.1152/jappl.1967.22.2.316>
- Hollenhorst, M.I., Jurastow, I., Nandigama, R., Appenzeller, S., Li, L., Vogel, J. et al. (2020) Tracheal brush cells release acetylcholine in response to bitter tastants for paracrine and autocrine signaling. *The FASEB Journal*, 34, 316–332. <https://doi.org/10.1096/fj.201901314RR>
- Horner, R.L., Innes, J.A., Holden, H.B. & Guz, A. (1991) Afferent pathway(s) for pharyngeal dilator reflex to negative pressure in man: A study using upper airway anaesthesia. *Journal of Physiology*, 436, 31–44. <https://doi.org/10.1113/jphysiol.1991.sp018537>
- Kanamaru, A., Mutoh, T., Kojima, K., Nishimura, R., Sasaki, N., Kuwahara, M. et al. (1999) The posterior nasal nerve plays an important role on cardiopulmonary reflexes to nasal application of capsaicin, distilled water and *l*-menthol in anesthetized dogs. *Journal of Veterinary Medical Science*, 61, 85–88. <https://doi.org/10.1292/jvms.61.85>
- Kinnamon, S.C. & Finger, T.E. (2013) A taste for ATP: Neurotransmission in taste buds. *Frontiers in Cellular Neuroscience*, 7, 264. <https://doi.org/10.3389/fncel.2013.00264>
- Klein, P.B. & Schroeder, H.E. (1979) Epithelial differentiation and taste buds in the soft palate of the monkey, *Macaca irus*. *Cell and Tissue Research*, 196, 181–188. <https://doi.org/10.1007/BF00236359>
- Krasteva, G. & Kummer, W. (2012) “Tasting” the airway lining fluid. *Histochemistry and Cell Biology*, 138, 365–383. <https://doi.org/10.1007/s00418-012-0993-5>
- Lalonde, E.R. & Eglitis, J.A. (1961) Number and distribution of taste buds on the epiglottis, pharynx, larynx, soft palate and uvula in a human newborn. *Anatomical Record*, 140, 91–95. <https://doi.org/10.1002/ar.1091400204>
- Lee, L.Y. (2009) Respiratory sensations evoked by activation of bronchopulmonary C-fibers. *Respiratory Physiology & Neurobiology*, 167, 26–35. <https://doi.org/10.1016/j.resp.2008.05.006>
- Lee, R.J., Kofonow, J.M., Rosen, P.L., Siebert, A.P., Chen, B., Doghramji, L. et al. (2014) Bitter and sweet taste receptors regulate human upper respiratory innate immunity. *Journal of Clinical Investigation*, 124, 1393–1405. <https://doi.org/10.1172/JCI72094>
- Lee, R.J., Xiong, G., Kofonow, J.M., Chen, B., Lysenko, A., Jiang, P. et al. (2012) T2R38 taste receptor polymorphisms underlie susceptibility

- to upper respiratory infection. *Journal of Clinical Investigation*, 122, 4145–4159. <https://doi.org/10.1172/JCI64240>
- Lin, W., Ogura, T., Margolskee, R.F., Finger, T.E. & Restrepo, D. (2008) TRPM5-expressing solitary chemosensory cells respond to odorous irritants. *Journal of Neurophysiology*, 99, 1451–1460. <https://doi.org/10.1152/jn.01195.2007>
- Liu, C., Kershberg, L., Wang, J., Schneeberger, S. & Kaeser, P.S. (2018) Dopamine secretion is mediated by sparse active zone-like release sites. *Cell*, 172, 706–718.e15. <https://doi.org/10.1016/j.cell.2018.01.008>
- Lundblad, L., Lundberg, J.M., Brodin, E. & Änggård, A. (1983) Origin and distribution of capsaicin-sensitive substance P-immunoreactive nerves in the nasal mucosa. *Acta Oto-Laryngologica*, 96, 485–493. <https://doi.org/10.3109/00016488309132735>
- Masuda, H., Nakamuta, N. & Yamamoto, Y. (2019) Morphology of GNAT3-immunoreactive chemosensory cells in the rat larynx. *Journal of Anatomy*, 234, 149–164. <https://doi.org/10.1111/joa.12914>
- Merigo, F., Benati, D., Tizzano, M., Osculati, F. & Sbarbati, A. (2005) α -Gustducin immunoreactivity in the airways. *Cell and Tissue Research*, 319, 211–219. <https://doi.org/10.1007/s00441-004-1007-2>
- Miura, H., Nakayama, A., Shindo, Y., Kusakabe, Y., Tomonari, H. & Harada, S. (2007) Expression of gustducin overlaps with that of type III IP3 receptor in taste buds of the rat soft palate. *Chemical Senses*, 32, 689–696. <https://doi.org/10.1093/chemse/bjm036>
- Miyazaki, J., Shin, T., Murata, Y. & Masuko, S. (1999) Pharyngeal branch of the vagus nerve carries intraepithelial afferent fibers in the cat pharynx: An elucidation of the origin and central and peripheral distribution of these components. *Otolaryngology - Head and Neck Surgery*, 120, 905–913. [https://doi.org/10.1016/S0194-5998\(99\)70335-9](https://doi.org/10.1016/S0194-5998(99)70335-9)
- Ohkuri, T., Horio, N., Stratford, J.M., Finger, T.E. & Ninomiya, Y. (2012) Residual chemoresponsiveness to acids in the superior laryngeal nerve in “taste-blind” (P2X2/P2X3 double-KO) mice. *Chemical Senses*, 37, 523–532. <https://doi.org/10.1093/chemse/bjs004>
- Perniss, A., Liu, S., Boonen, B., Keshavarz, M., Ruppert, A.-L., Timm, T. et al. (2020) Chemosensory cell-derived acetylcholine drives tracheal mucociliary clearance in response to virulence-associated formyl peptides. *Immunity*, 52, 683–699. <https://doi.org/10.1016/j.immuni.2020.03.005>
- Roper, S.D. (2013) Taste buds as peripheral chemosensory processors. *Seminars in Cell & Developmental Biology*, 24, 71–79. <https://doi.org/10.1016/j.semcdb.2012.12.002>
- Sbarbati, A., Merigo, F., Benati, D., Tizzano, M., Bernardi, P., Crescimanno, C. et al. (2004) Identification and characterization of a specific sensory epithelium in the rat larynx. *The Journal of Comparative Neurology*, 475, 188–201. <https://doi.org/10.1002/cne.20172>
- Sekerková, G., Freeman, D., Mugnaini, E. & Bartles, J.R. (2005) Espin cytoskeletal proteins in the sensory cells of rodent taste buds. *Journal of Neurocytology*, 34, 171–182. <https://doi.org/10.1007/s11068-005-8352-2>
- Shah, A.S., Ben-Shahar, Y., Moninger, T.O., Kline, J.N. & Welsh, M.J. (2009) Motile cilia of human airway epithelia are chemosensory. *Science*, 325, 1131–1134. <https://doi.org/10.1126/science.1173869>
- Spina, D. (1996) Airway sensory nerves: A burning issue in asthma? *Thorax*, 51, 335–337. <https://doi.org/10.1136/thx.51.3.335>
- Stjärne, P., Lundblad, L., Änggård, A., Hökfelt, T. & Lundberg, J.M. (1989) Tachykinins and calcitonin gene-related peptide: Co-existence in sensory nerves of the nasal mucosa and effects on blood flow. *Cell and Tissue Research*, 256, 439–446. <https://doi.org/10.1007/BF00225591>
- Takahashi, N., Nakamuta, N. & Yamamoto, Y. (2016) Morphology of P2X3-immunoreactive nerve endings in the rat laryngeal mucosa. *Histochemistry and Cell Biology*, 145, 131–146. <https://doi.org/10.1007/s00418-015-1371-x>
- Tanaka, Y., Yoshida, Y., Hirano, M., Morimoto, M. & Kanaseki, T. (1987) Intramucosal distribution of the glossopharyngeal sensory fibers of cats. *Brain Research Bulletin*, 19, 115–127. [https://doi.org/10.1016/0361-9230\(87\)90174-2](https://doi.org/10.1016/0361-9230(87)90174-2)
- Terenghi, G., Polak, J.M., Rodrigo, J., Mulderry, P.K. & Bloom, S.R. (1986) Calcitonin gene-related peptide-immunoreactive nerves in the tongue, epiglottis and pharynx of the rat: Occurrence, distribution and origin. *Brain Research*, 365, 1–14. [https://doi.org/10.1016/0006-8993\(86\)90716-X](https://doi.org/10.1016/0006-8993(86)90716-X)
- Tizzano, M., Cristofolletti, M., Sbarbati, A. & Finger, T.E. (2011) Expression of taste receptors in solitary chemosensory cells of rodent airways. *BMC Pulmonary Medicine*, 11, 3. <https://doi.org/10.1186/1471-2466-11-3>
- Tizzano, M. & Finger, T.E. (2013) Chemosensors in the nose: Guardians of the airways. *Physiology (Bethesda)*, 28, 51–60. <https://doi.org/10.1152/physiol.00035.2012>
- Tizzano, M., Gulbrandsen, B.D., Vandenbeuch, A., Clapp, T.R., Herman, J.P., Sibhatu, H.M. et al. (2010) Nasal chemosensory cells use bitter taste signaling to detect irritants and bacterial signals. *Proceedings of the National Academy of Sciences of the United States of America*, 107, 3210–3215. <https://doi.org/10.1073/pnas.0911934107>
- Travers, S.P. & Nicklas, K. (1990) Taste bud distribution in the rat pharynx and larynx. *Anatomical Record*, 227, 373–379. <https://doi.org/10.1002/ar.1092270313>
- Uddman, R., Luts, A. & Sundler, F. (1985) Occurrence and distribution of calcitonin gene-related peptide in the mammalian respiratory tract and middle ear. *Cell and Tissue Research*, 241, 551–555. <https://doi.org/10.1007/BF00214575>
- Winkelman, V.E., Thompson, K.E., Neuland, K., Jaramillo, A.M., Fois, G., Schmidt, H. et al. (2019) Inflammation-induced upregulation of P2X4 expression augments mucin secretion in airway epithelia. *American Journal of Physiology. Lung Cellular and Molecular Physiology*, 316, L58–L70. <https://doi.org/10.1152/ajplung.00157.2018>
- Yang, R., Crowley, H.H., Rock, M.E. & Kinnamon, J.C. (2000) Taste cells with synapses in rat circumvallate papillae display SNAP-25-like immunoreactivity. *The Journal of Comparative Neurology*, 424, 205–215. [https://doi.org/10.1002/1096-9861\(20000821\)424:2%3C205:AID-CNE2%3E3.0.CO;2-F](https://doi.org/10.1002/1096-9861(20000821)424:2%3C205:AID-CNE2%3E3.0.CO;2-F)

How to cite this article: Yamamoto Y, Yokoyama T, Nakamuta N. Morphology of GNAT3-immunoreactive chemosensory cells in the nasal cavity and pharynx of the rat. *J Anat.* 2021;239:290–306. <https://doi.org/10.1111/joa.13424>